

Human activity patterns in cities on a planetary scale: A network science and machine learning approach

Francisco Betancourt^{1,+,*}, Alejandro P. Riascos^{1,+}, and José L. Mateos^{1,2,+}

¹Instituto de Física, Universidad Nacional Autónoma de México, Ciudad Universitaria, 04510 Ciudad de México, México.

²Centro de Ciencias de la Complejidad, Universidad Nacional Autónoma de México, 04510 Ciudad de México, México.

*email: cfrancisco@ciencias.unam.mx

+These authors contributed equally to this work

ABSTRACT

In this work, we aim at studying the diversity of human activity patterns in cities around the world. In order to do so, we use, as a proxy, the data provided by the online location-based social network Foursquare, where users make check-ins that indicate points of interest in the city. The data set comprise more than 90 million check-ins in 632 cities of 84 countries in 5 continents. We analyzed more than 11 million points of interest including all sort of places: airports, train stations, restaurants, cafes, bars, parks, hospitals, gyms and many others. With this information we obtained spatial and temporal patterns of activities of each city. We quantify similarities and differences of these patterns for all the cities involved, and construct a network connecting pairs of cities. The links of this network indicate the similarity of patterns between cities and is quantified with the relative entropy between two distributions. Then, we obtained the community structure of this network and the geographic distribution of communities. For comparison, we use a Machine Learning algorithm - unsupervised agglomerative clustering - to obtained clusters or communities of cities with similar patterns. The main result is that both approaches give the same classification of five communities belonging to five different continents worldwide. This suggest that human activity patterns can be universal with some geographical, historical and cultural variations on a planetary scale.

Introduction

In recent years, cities have become a topic of considerable scientific interest¹⁻³ since more than half of the population live in urban areas¹. This worldwide tendency of humans to migrate from rural areas to cities is due to the fact that, in general, people find more opportunities to develop in their living standards.

In the last decade, the development of technologies for practically all aspects of urban life has made available an unprecedented amount of data that provides information related to almost any process and activity carried out by people in cities⁴. Banking data (bill-tracking⁵, electronic banking, credit card transactions⁶, network ATMs), surveys and censuses⁷⁻⁹, public and private transportation services (buses¹⁰, taxis¹¹, subways¹², transport apps, bicycle and like loan systems¹³), telecommunications networks (cell phones¹⁴⁻²¹, GPS devices²²⁻²⁵), applications and devices for multiple everyday purposes (internet of things, emails, navigation applications, messaging, social networks); all of these digital traces make it possible to investigate the human activity in urban areas quantitatively, in an interdisciplinary fashion.

A very important source of information for the study of human behavior in cities are Location-Based Social Networks (LBSN)²⁶. In these, people share information about the places they visit and that may be of interest to the user community. These venues, which throughout this work we will call as Points of Interest (POIs), are identifiable within the platform and one advantage is that the user can search for them based on categories (restaurants, entertainment, health, etc.) and based on physical proximity, using the geolocation of the devices, such as SmartPhones, for example. LBSN provide valuable information on the interactions of two kinds of entities that make up cities: people and physical places. This is why this interplay has been explored in studies of urban mobility²⁷, human behavior^{28,29}, social interactions and encounter networks^{30,31}.

In this study we use data from Foursquare³², a location-based social network that has been used previously in some studies^{30,31,33-40}. A more detail description of Foursquare will be given in the next sections. A highly relevant aspect of human

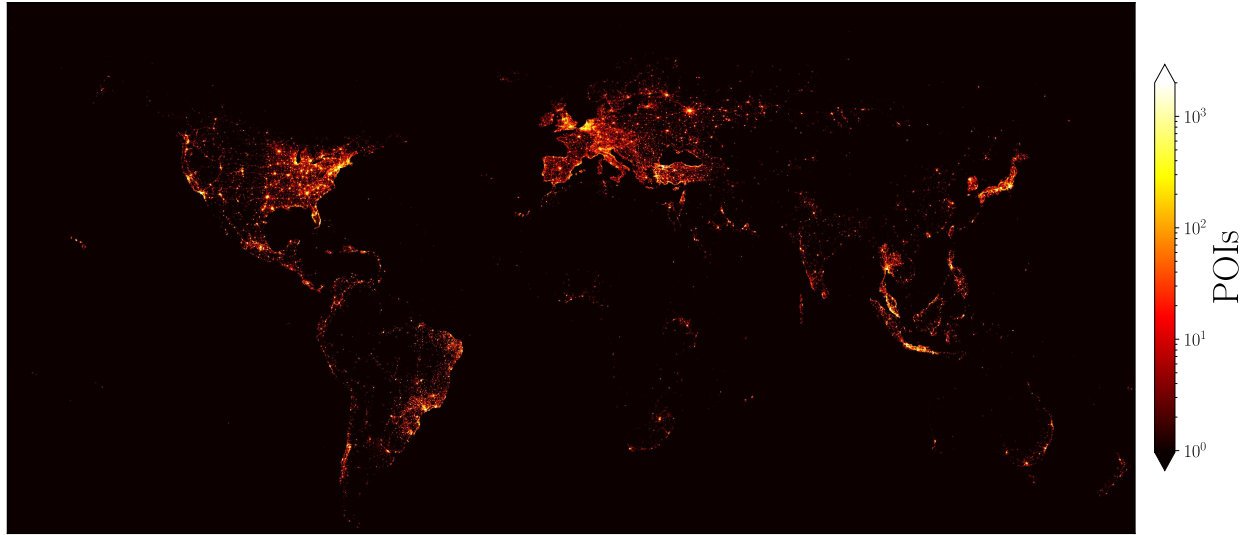


Figure 1. Points of interest worldwide from human activity in Foursquare. This analysis includes 11,179,790 points of interest (POIs). The counts codified in the colorbar show the number of POIs in each rectangle of a grid from -180° to 180° in the longitude and from -56° to 85° in the latitude (the dimensions of the grid are $3,600 \times 1,410$ squares defined by sides with 0.1°). A logarithmic scale was used to show the non-null frequencies of POIs found in the squares; the zones with null counts of POIs are depicted in black. This representation only considers geographical information of POIs, no map was used for this analysis. This figure was created using python 3.8 and the matplotlib (3.5.0) package (<https://matplotlib.org>).

activity and mobility in cities is its time dimension. This has been addressed through the use of different sources such as emails⁴¹, phone call records⁴², data from official sources⁴³ and analysis of activity in POIs and LBSN⁴⁴, among others. Here, we will study human activity patterns in cities around the world. The data comprise more than 11 million POIs of 632 cities in 84 countries located in 5 continents. With this information we obtained spatial and temporal patterns of activities of each city. In this work, we will focus mainly in the temporal patterns of activities on a weekly basis. We quantify similarities and differences of these patterns for all the cities involved, and generate a network⁴⁵ that links pairs of cities. The links indicate the similarity of patterns between cities and is quantified with the relative entropy (Kullback-Leibler divergence)⁴⁶ between the corresponding distributions. Then, we obtained the community structure of this network and the geographic distribution of communities. On the other hand, we use a Machine Learning approach to classify the clusters in the data. In particular, we used the unsupervised agglomerative hierarchical clustering algorithm to obtained clusters or communities of cities with similar patterns⁴⁷. Both approaches give a very similar classification of five communities that distribute geographically in five different continents throughout the world.

Results

Check-ins and points of interest in Foursquare

In this work, we use Foursquare check-ins as a proxy of human activity in cities. Check-ins are spatio-temporal interactions between users and points of interest (POIs). They provide vast information about people's interests, site characteristics, and behavioral patterns in cities, among many others. This is why Foursquare metadata and location-based social networks in general, can provide useful information for studies of mobility, infrastructure, human behavior, and public policy, just to mention a few examples.

We study a large-scale and long-term Foursquare data set collected by Yang et al.^{30,35} that is publicly available⁴⁸. The data set contains 90,048,627 check-ins made by 2,733,324 users from April 2012 to January 2014. The authors collected active check-ins from Twitter by searching a hashtag generated automatically for users that linked their Foursquare activity with that social network. Then, with the set of places where venues occurred, they collected the POIs description; this information is available to the public from the Foursquare platform. The records include detailed information about the POIs, their coordinates, and the exact time of each user check-in^{30,35}. In this manner, the dataset provides the space-temporal activity obtained from the sequence of successive check-ins for each user. Furthermore, the registers include a short description that labels each POI

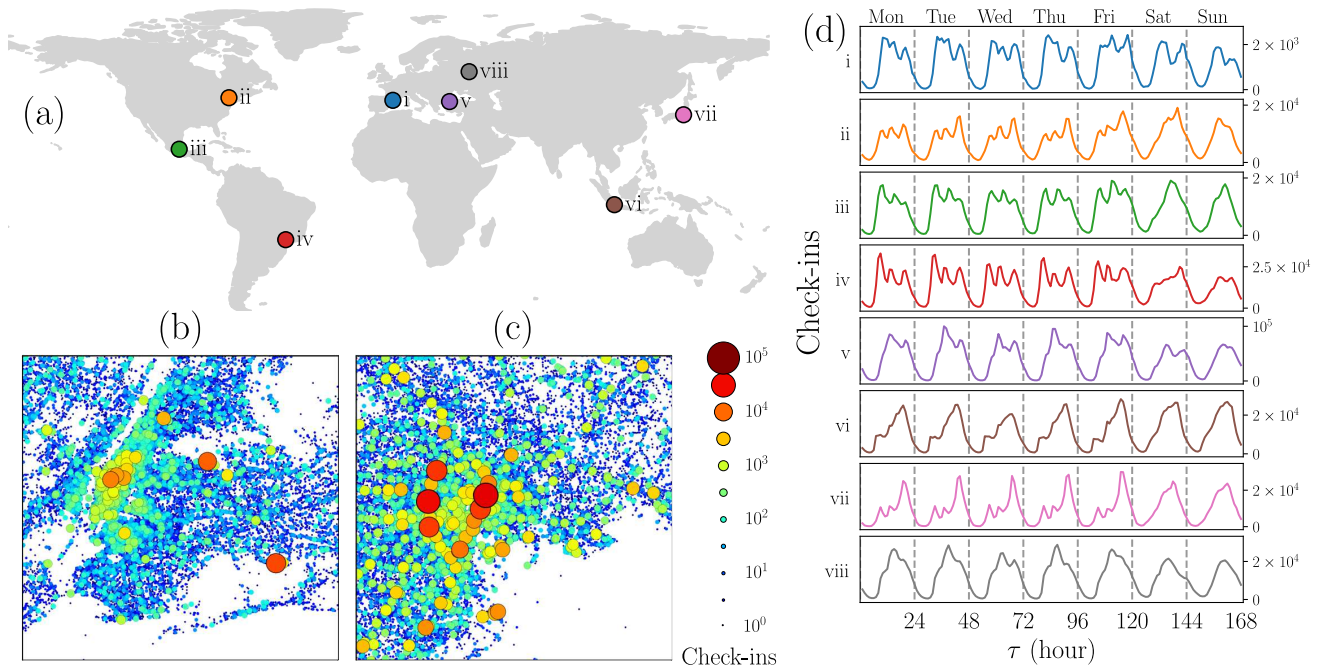


Figure 2. Spatial and temporal analysis of check-ins in different cities. (a) Eight selected cities: (i) Barcelona, (ii) New York, (iii) Mexico City, (iv) Sao Paulo, (v) Istanbul (vi), Jakarta, (vii) Tokyo, and (viii) Moscow. Points of interest in the Foursquare dataset in New York (b) and Tokyo (c). In this representation, the color and area of the circles denote the number of check-ins in the respective POI. (d) All the check-ins in the cities (i) to (viii) presented in (a) were gathered using the local time when they were made. The counts reported in the histograms correspond to the number of check-ins in each hour of the week, from the first hour on Monday to the last hour on Sunday. All figures were created using python 3.8 and the matplotlib (3.5.0) package (<https://matplotlib.org>). The map in panel (a) was created using the geopandas (0.12.1) package (<https://geopandas.org>).

with specific keywords (for example “restaurant”, “metro”, “university”) and a social network of users defined via the mutual following between Twitter accounts. We did not incorporate this information in our study (see the methods section for a detailed description of the data).

The complete dataset includes information of Foursquare users in every country in the world. From the 253 country codes, check-ins on 84 countries with 5000 or more POIs represent 98.92% of data. To visualize the geographical distribution of the POIs worldwide, we grouped them according to their coordinates. We generate a two-dimensional histogram dividing the latitude and longitude using square bins with side 0.1° and counting the number of POIs in each coordinate square. This allowed us to identify regions with non-null POIs and those with the highest concentration. In Fig. 1 we depict the spatial distribution obtained; it consists of 3600×1410 squares covering latitudes from -56.6° and 84.6° , and longitudes from -180° to 180° ; latitudes excluded are due to the lack of POIs on those regions. The number of POIs in each region is codified in the colorbar, where a logarithmic scale was chosen to show the wide range of values. The great coverage of this dataset is clear, as well as the existence of regions with high concentrations of POIs reaching up to 70,128 POIs in a single square defined above. The plot is the result of projecting the coordinates of the globe on a rectangle which implies spatial distortions; still, the frontiers of continents are identifiable even though no borders were used or drawn. A high density of POIs can be appreciated in North America and Europe, but active regions are also present in South America, the Middle East, and East Asia. Although to a much lesser extent, there are some localized regions with high numbers of POIs in Africa and Oceania. The details of this information are discussed in the methods section in Table 1, where the 15 countries with most of the POIs are listed; 80% of the venues belong to these countries.

Temporal activity of users in Foursquare

The classification of POIs and check-ins at the level of cities allows us to perform temporal, spatial and, spatio-temporal analysis of features. For example, in Ref.³¹ a detailed study of the activity in Foursquare, of users in New York and Tokyo, is presented. In Fig. 2 we illustrate spatial and temporal analysis in different cities. In Fig. 2(a) we show in a map eight cities representing different regions of the world: (i) Barcelona (Spain), (ii) New York (United States), (iii) Mexico City (Mexico),

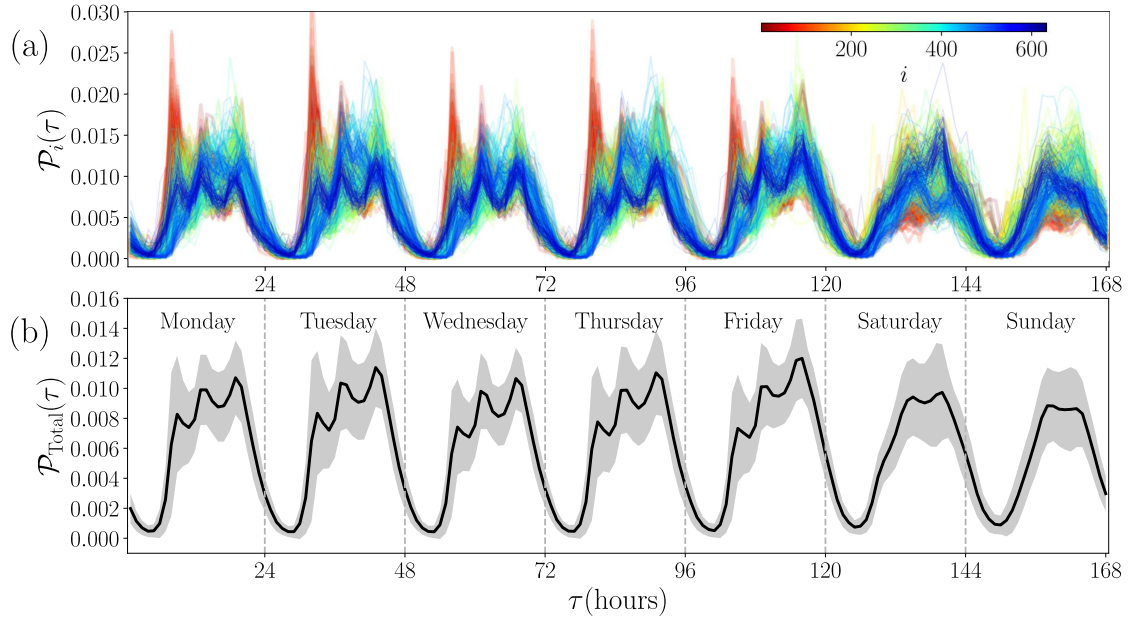


Figure 3. Temporal analysis of check-ins in 632 cities. (a) Probability $\mathcal{P}_i(\tau)$ of check-in at times τ in $N = 632$ cities denoted by $i = 1, 2, \dots, N$. All the check-ins in each city were gathered by the local time when each venue was made. Frequency counts are normalized over the week to obtain each $\mathcal{P}_i(\tau)$. The time τ can take the values from 1 (the first hour of Monday) to 168 (the last hour of Sunday), and the results for each city i (codified in the colorbar) are presented with continuous lines. (b) The probability $\mathcal{P}_{\text{Total}}(\tau)$ obtained for all the check-ins in the 632 cities is plotted with a continuous line. In this case, the standard deviation $\sigma(\tau)$ for all the check-ins and all the cities in (a) evaluated at time τ defines variations of this probability. The results are shown as a region defined by $\mathcal{P}_{\text{Total}}(\tau) \pm \sigma(\tau)$ presented with gray color. All figures were created using python 3.8 and the matplotlib (3.5.0) package (<https://matplotlib.org>).

(iv) Sao Paulo (Brasil), (v) Istanbul (Turkey), (vi) Jakarta (Indonesia), (vii) Tokyo (Japan), and (viii) Moscow (Russia). In Figs. 2(b)-(c), we show the spatial distribution of POIs for two cities, in combination with their attractiveness, measured as their number of check-ins for New York and Tokyo. The results reveal characteristics of a complex urban environment in which most POIs register a lower number of check-ins while a few POIs have an attractiveness several orders of magnitude greater. A similar result has been reported by Yang et al.³⁰, at a global scale for the same dataset. This power-law behavior in the attractiveness of POIs is also observed at different scales in other studies; for example, in the attractiveness of sites measured from the activity of taxis in New York City¹¹ or the importance of airports in the United States⁴⁹. In this context, our findings in Fig. 2(b)-(c) show that the activity of users in Foursquare is associated with the complexity in the distribution of POIs. This feature is observed in all the cities in this study.

In Fig. 2(d) we present the temporal analysis of user activity in the eight cities shown in Fig. 2(a). Temporal information of the check-ins was grouped by urban area and was generated using the local time, obtained through the Universal Coordinated Time and adding the minutes corresponding to the timezone correction (see methods section for details). In this way, we can identify daily routines for many geographical areas around the world. For this study, we defined the time granularity as 168 hours (corresponding to a full week), so we have, for each region, a histogram with all the check-ins made in the period of observation gathered by hour. We considered this histogram as a characteristic print of human temporal activity within a region. In doing so, clear patterns emerge with slight differences between regions. Some regularities are evident: there is low activity of check-ins during the night and high activity during the day; again, this matches the behavior reported by Yang, et al.³⁰, for a subset of this data at a global scale. In this case, the pattern persists at a local scale, as has been shown for other phenomena^{21,43,44}. But, at this level, differences in patterns become noticeable; the part of the day that concentrates most of the activity, the maximum number of check-ins in a day, and the change of the activity patterns for weekdays and weekends describes the collective behavior of city inhabitants that varies from one city to another.

In Fig. 3 we extend the temporal analysis of check-ins to $N = 632$ cities in 84 countries. We consider activity counts as in panels in Fig. 2(d), all the information of check-ins in a city i were gathered using the corresponding local time τ . The activity counts are normalized over the week to obtain the relative frequency or probability $\mathcal{P}_i(\tau)$. The time τ can take the values from

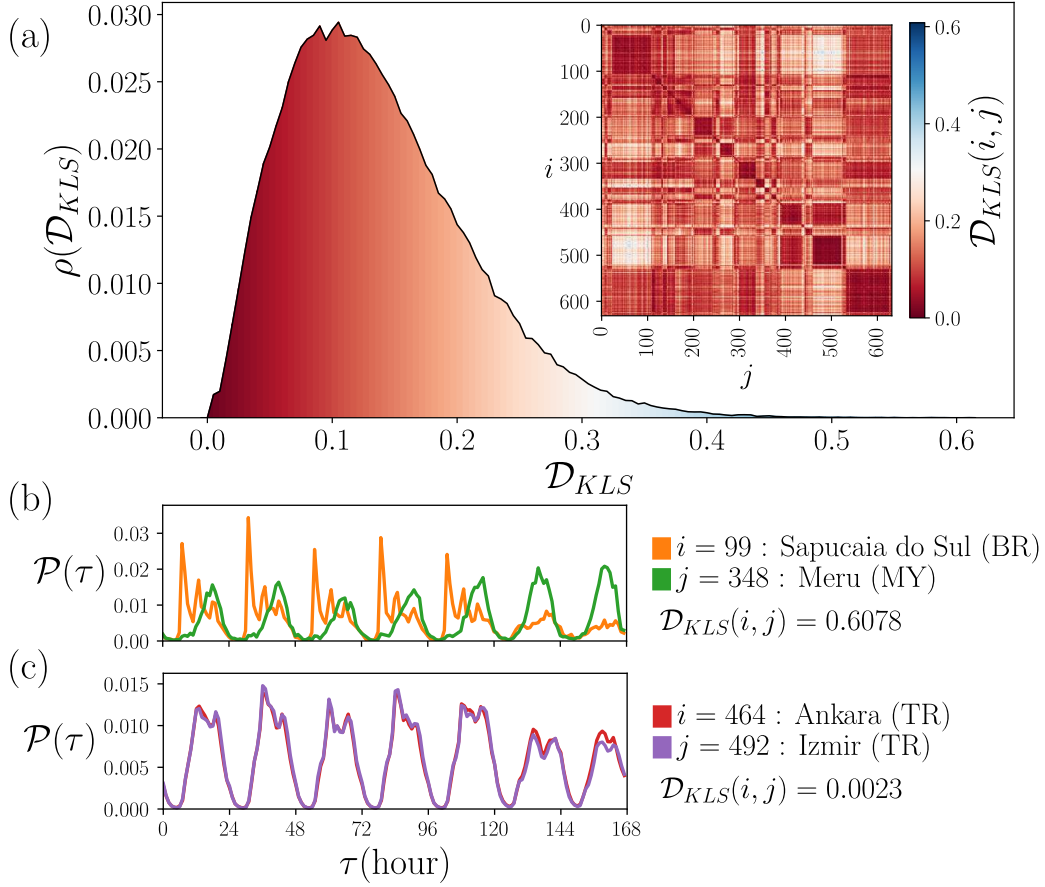


Figure 4. Comparison of temporal activity between cities. (a) Statistical analysis of the symmetric Kullback-Leibler distances \mathcal{D}_{KLS} from the comparison of check-ins temporal distribution by pairs. The values are obtained from Eq. (3) for all the city pairs $i, j = 1, \dots, 632$. The probability density $\rho(\mathcal{D}_{KLS})$ is obtained using bin counts in intervals with $\Delta\mathcal{D}_{KLS} = 0.005$. The matrix with all the elements $\mathcal{D}_{KLS}(i, j)$ is presented as an inset. (b) The two most different probability densities of the set are of the cities Sapucaia do Sul in Brazil and Meru in Malaysia, with $\mathcal{D}_{KLS} = 0.6078$; the maximum value found. (c) The two most similar cities of our sample, are Ankara and Izmir both in Turkey, with $\mathcal{D}_{KLS} = 0.0023$, the minimum non-null value. All figures were created using python 3.8 and the matplotlib (3.5.0) package (<https://matplotlib.org>).

1 (associated to the first hour of Monday) to 168 (the last hour of Sunday). In Fig. 3(a), we present the probability $\mathcal{P}_i(\tau)$ of check-in at times τ in cities denoted by $i = 1, 2, \dots, 632$. The results reveal marked differences between low nocturnal activity and high daytime activity. Also, patterns emerge in all of them by grouping check-ins by their local time τ of occurrence. For all the cities, fluctuations in the values of $\mathcal{P}_i(\tau)$ are small at night, but during the day we see different behaviors of the curves describing each city with all kinds of deviations; for example, in some cities $\mathcal{P}_i(\tau)$ changes considerably in the early hours of the morning, others at night, whereas other cities differ considerably at weekends. To show these variations more clearly, in Fig 3(b) we depict $\mathcal{P}_{\text{Total}}(\tau)$, obtained for all the check-ins in the $N = 632$ cities. This quantity is equivalent to calculate the average between all cities

$$\mathcal{P}_{\text{Total}}(\tau) = \frac{1}{N} \sum_{i=1}^N \mathcal{P}_i(\tau). \quad (1)$$

On the other hand, the respective standard deviation $\sigma(\tau)$ of the values $\mathcal{P}_i(\tau)$ give us a measure of the differences observed in the cities considered. Our findings are shown in Fig. 3(b) as a shaded region defined by $\mathcal{P}_{\text{Total}}(\tau) \pm \sigma(\tau)$. The dispersion of the values in particular hours of the day can be seen, and noticeable variations between week days and weekends can be observed.

Comparison of temporal activity between cities using the Kullback-Leibler divergence

The variety of results observed for the probabilities $\mathcal{P}_i(\tau)$ in Fig. 3(a) motivates the exploration of a criterion to compare the temporal activity between two particular cities i, j . To this end, we use the Kullback-Leibler divergence, also known as the relative entropy, defined by^{46,50}

$$\mathcal{D}_{KL}(i, j) = \sum_{\tau} \mathcal{P}_i(\tau) \log \left[\frac{\mathcal{P}_i(\tau)}{\mathcal{P}_j(\tau)} \right], \quad (2)$$

where the sum in time τ ranges from 1 to 168 (all the hours in a week) and $i, j = 1, 2, \dots, N$. This divergence $\mathcal{D}_{KL}(i, j)$ compares $\mathcal{P}_i(\tau)$ using as a reference $\mathcal{P}_j(\tau)$; in particular, $\mathcal{D}_{KL}(i, j) = 0$ if $\mathcal{P}_i(\tau)$ and $\mathcal{P}_j(\tau)$ are equal. In other cases, $\mathcal{D}_{KL}(i, j) > 0$. However, the Kullback-Leibler divergence is not a distance since $\mathcal{D}_{KL}(i, j)$ is different from $\mathcal{D}_{KL}(j, i)$. To recover this symmetry, we used a symmetric version $\mathcal{D}_{KLS}(i, j)$, defined by

$$\mathcal{D}_{KLS}(i, j) \equiv \frac{\mathcal{D}_{KL}(i, j) + \mathcal{D}_{KL}(j, i)}{2}. \quad (3)$$

In Fig. 4, we present the results obtained from the evaluation of $\mathcal{D}_{KLS}(i, j)$, in Eq. (3), to compare the temporal activity presented in Fig. 3(a) for all the cities $i, j = 1, 2, \dots, 632$, considering the information of user's check-ins in Foursquare. In Fig. 4(a) we present the statistical analysis of $\mathcal{D}_{KLS}(i, j)$ for all pairs of cities. The results are depicted as a probability density $\rho(\mathcal{D}_{KLS})$ for the values \mathcal{D}_{KLS} , that is, we calculate the values of $\mathcal{D}_{KLS}(i, j)$ for all the pairs (i, j) . With these values, we obtained the histogram shown. We show, as an inset, the $N \times N$ matrix with elements $\mathcal{D}_{KLS}(i, j)$; the respective values are codified in the colorbar. The results for $\rho(\mathcal{D}_{KLS})$ show that a high fraction of the entries in the matrix have values \mathcal{D}_{KLS} around 0.1. For the diagonal elements we have $\mathcal{D}_{KLS}(i, i) = 0$. On the other hand, the maximum value for two different cities is $\mathcal{D}_{KLS} = 0.6078$, and occurs between the Brazilian city of Sapucaia do Sul and Meru, in Malaysia, as shown in Fig. 4(b). At the opposite extreme, the minimum non-null value reached is $\mathcal{D}_{KLS} = 0.0023$, found for the comparison between Ankara and Izmir, both in Turkey. The respective probabilities are shown in Fig. 4(c). The results observed in Fig. 4(b) are reasonable since we are comparing the activity in two complete different urban areas. In contrast, for the cities considered in Fig. 4(c), the resemblance between these two cities is remarkable considering that they are more than 520 km apart. Additionally, a review of the data shows that of the 82,285 active users in Ankara and the 90,923 active users in Izmir, only 11,141 made check-ins in both cities; this represents only 6.87% of the total users with activity in these regions. The similarity in their patterns is not explained by common users but by comparable urban behavior in the same country.

Networks and temporal patterns between cities

In this section, we apply methods of network science to analyze the similarities between cities. To this end, we define a network in which nodes represent cities and links the similarity relationship between cities. In this way, two nodes are connected if the respective cities have similar temporal activity. To generate this structure, it is necessary to define what is considered sufficiently similar. We use a threshold value H . If two cities have values \mathcal{D}_{KLS} in Eq. (3) lower or equal than H then these cities are considered similar. All this information defines a similarity network for each value H . The respective $N \times N$ adjacency matrix is denoted as $\mathbf{A}(H)$, with elements i, j given by

$$A_{ij}(H) = \begin{cases} 1 & \mathcal{D}_{KLS}(i, j) \leq H, \\ 0 & \text{otherwise.} \end{cases} \quad (4)$$

Additionally, we require $A_{ii}(H) = 0$ for $i = 1, 2, \dots, N$, to avoid self loops. From the symmetry of the distance \mathcal{D}_{KLS} , follows the symmetry of $\mathbf{A}(H)$, defining an undirected network.

In Fig. 5, we analyze similarity networks as a function of H . In Fig. 5(a) we depict the adjacency matrix $\mathbf{A}(H)$ for different values of H . In this manner, for each H all the information of $\mathcal{D}_{KLS}(i, j)$ in Fig. 4(a) is converted into a binary matrix with entries 0 and 1. In Fig. 5(b), we present the fraction of nodes $v_{LCC} = S_{LCC}/N$, where S_{LCC} is the size of the Largest Connected Component (LCC). The LCC obtained for the values of H explored in Fig. 5(a) are shown as insets.

In the results in Fig. 5(b), it is worth noticing that for $H = 0.005$, the network is formed by disconnected subnetworks with a few nodes and the LCC is a linear graph with 6 nodes; for $H < 0.0023$ each node is disconnected. On the other hand, the network is fully connected for $H > 0.6078$; the maximum value of \mathcal{D}_{KLS} found. The transition between these two limits gives rise to a convenient choice of H corresponding with a network that captures the nature of the similarity between the cities that we are analyzing. The results for v_{LCC} reveal that the size of the LCC contains more than 90% of the nodes at $H = 0.031$, 99% at $H = 0.052$. On the other hand, $H = 0.0723$ is the minimal value of the similarity threshold that produces a connected network that includes all the $N = 632$ nodes (cities). Finally, we see that around $H = 0.02$, v_{LCC} suffers an abrupt change with

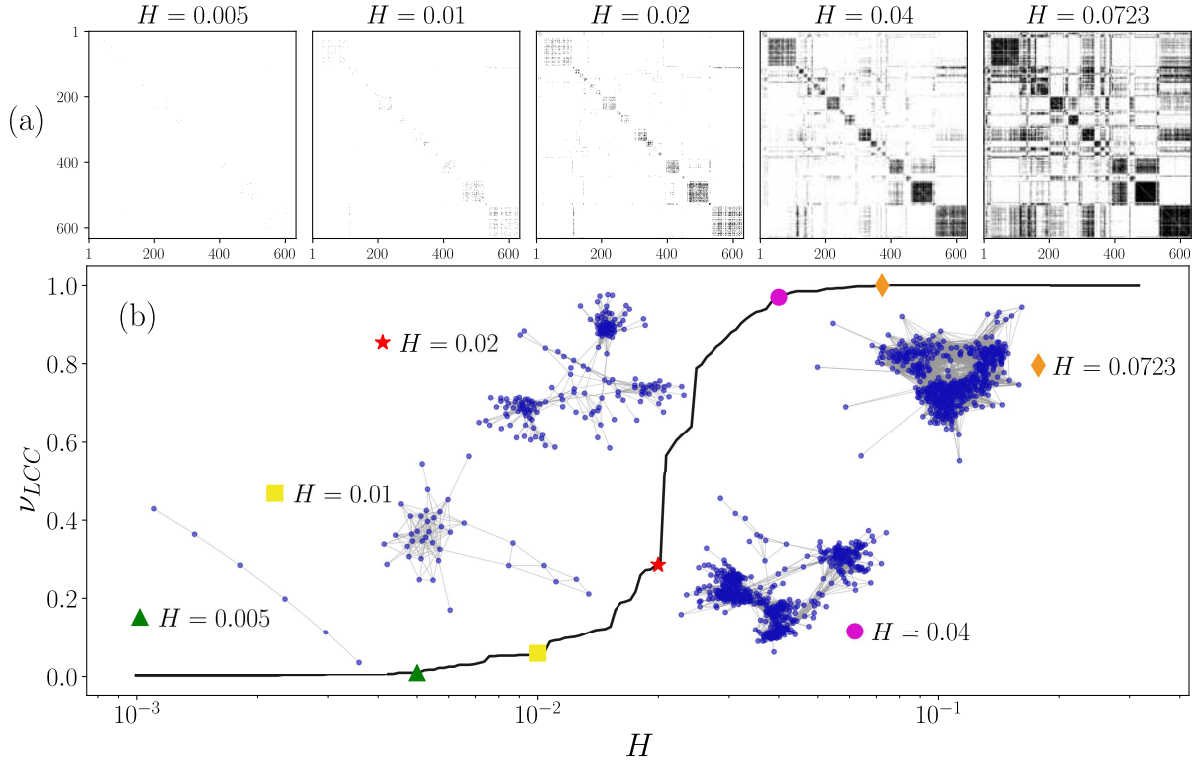


Figure 5. Similarity networks generated using different threshold values H . (a) Adjacency matrices $A(H)$ with elements given by Eq. (4) using the values $H \in \{0.005, 0.01, 0.02, 0.04, 0.0723\}$, binary entries $A_{ij}(H)$ are depicted in white for 0 and black for 1. (b) Fraction of nodes in the largest connected component v_{LCC} as a function of H in the interval $0.001 \leq H \leq 0.32$. The largest connected component of the networks generated with $A(H)$ in panel (a) are presented as inset. All figures were created using python 3.8 and the matplotlib (3.5.0) package (<https://matplotlib.org>).

H that is analogous to a percolation threshold⁴⁵, separating two regimes: one with $v_{LCC} < 0.3$, defining small sub-networks with high similarity in the temporal information and a second one with $v_{LCC} > 0.6$ where the connected networks incorporate a high fraction of the cities.

Once we established a criteria to build similarity networks using the temporal activity of users of Foursquare in Fig. 3(a), we can apply community detection algorithms. The concept of community has emerged in network science as a method for finding groups within complex systems identifying sub-networks with statistically significantly more links between nodes in the same group than nodes in different groups^{51–53}. In our similarity network, these communities represent groups of cities with comparable activity $\mathcal{P}_i(\tau)$. In Fig. 6 we present the results for a network with $N = 632$ nodes generated with $H = 0.0723$.

In panel 6(a) we depict five communities $\mathcal{C}_1, \mathcal{C}_2, \dots, \mathcal{C}_5$ detected using the Louvain’s algorithm⁵⁴ implemented in the library NetworkX in Python⁵⁵. The number of nodes on each community \mathcal{C}_s (with $s = 1, 2, \dots, 5$) is denoted by \mathcal{N}_s and, from this analysis we obtain groups of cities with $\mathcal{N}_1 = 148$, $\mathcal{N}_2 = 136$, $\mathcal{N}_3 = 133$, $\mathcal{N}_4 = 113$, and $\mathcal{N}_5 = 102$. In Fig. 6(b) we plot with thin gray lines the probabilities $\mathcal{P}_i(\tau)$ showed in Fig. 3(a) in groups defined by each community \mathcal{C}_s ; each panel contains \mathcal{N}_s curves. In addition, we include the statistical analysis considering all the check-ins in each group; the results are shown with colored thick lines. When grouped in this way, the curves observed within each community \mathcal{C}_s are similar, evidencing the fact that they have the same shape as the averages.

The average curves in Fig. 6(b) show that the \mathcal{C}_1 community, whose average is plotted in blue, has a behavior from Monday to Friday characterized by three peaks throughout the day (at 8, 12 and 18 hours). On weekends, this pattern is broken and a single maximum is observed around 20 hours on Saturday and at noon on Sunday. The \mathcal{C}_2 community, with the orange average line, is characterized by a pronounced maximum at 13 hours and a second relative maximum at 19 hours, from Monday to Friday. This behavior is maintained on weekends but with less check-ins. The community \mathcal{C}_3 , with a curve in green, is the one with the least contrast between the shape from weekdays versus weekends. Every day the maximum is found at 18 hours. Still, from Monday through Friday there is a small local maximum at 8 hours that disappears on the weekend. \mathcal{C}_4 with the average presented in red, has the same features as \mathcal{C}_1 but with different relative sizes; in this case, the first daily maximum

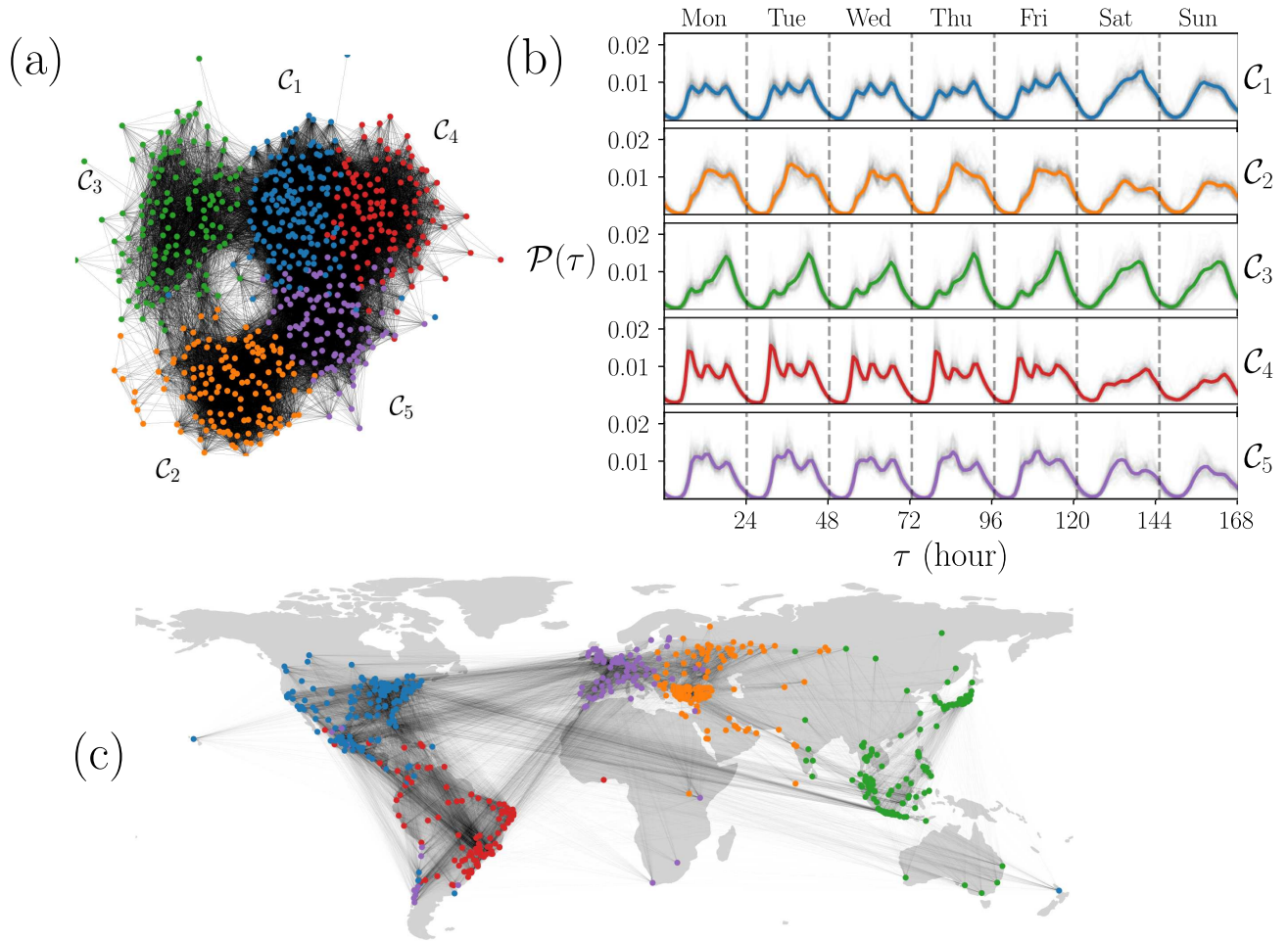


Figure 6. Human activity patterns identified using community detection in similarity networks. (a) Community structure of the similarity network generated with $H = 0.0723$, five communities $\mathcal{C}_1, \mathcal{C}_2, \mathcal{C}_3, \mathcal{C}_4, \mathcal{C}_5$ were detected using the Louvain's algorithm and are represented with different colors. (b) Probability $\mathcal{P}(\tau)$ for the temporal activity of the cities in each community. Thin gray lines present the curves $\mathcal{P}_i(\tau)$ depicted in Fig. 3(a) whereas the colored thick line represents the statistical analysis of all the check-ins in the cities of the community. (c) Geographical representation of the network in (a). In this case, each node is a city depicted on a world map. All figures were created using python 3.8 and the matplotlib (3.5.0) package (<https://matplotlib.org>). The map in panel (c) was created using the geopandas (0.12.1) package (<https://geopandas.org>).

dominates over the rest. The \mathcal{C}_5 community is the smallest and whose average behavior is depicted in purple. In this case the curve suffers different changes throughout the week. While there is a pattern with maxima at 9, 12 and 19 hours, and a valley at 15 hours, from Monday to Friday, the relative sizes are not always equal; on Monday the first and second peaks dominate, on Tuesday the second maximum is the largest, on Wednesday the three are practically the same size, on Thursday the first two peaks almost merge and dominate over the third, and on Friday the first almost disappears while the second peak dominates. Finally, on Saturday there is a change giving rise to two maximums at 13 and 20 hours, also present on Sunday although smaller.

In addition, considering that each probability curve $\mathcal{P}_i(\tau)$ corresponds to a node i , which in turn is a city with given coordinates, in Fig. 6(c) we plot the network with each node located in a world map. The node colors and the whole network connectivity are the same as in Fig. 6(a). This network representation shows that the communities formed from the similarity of city behaviors correspond to well-defined geographic regions. Cities in North America belong predominantly to the \mathcal{C}_1 community; those in Eastern Europe and the Middle East belong to \mathcal{C}_2 ; the \mathcal{C}_3 community is composed of several cities in Eastern India, and cities in East Asia and Oceania; \mathcal{C}_4 contains most cities in South America, and most of the cities in Western Europe belong to the \mathcal{C}_5 community. This is a remarkable result that we will discuss further below.

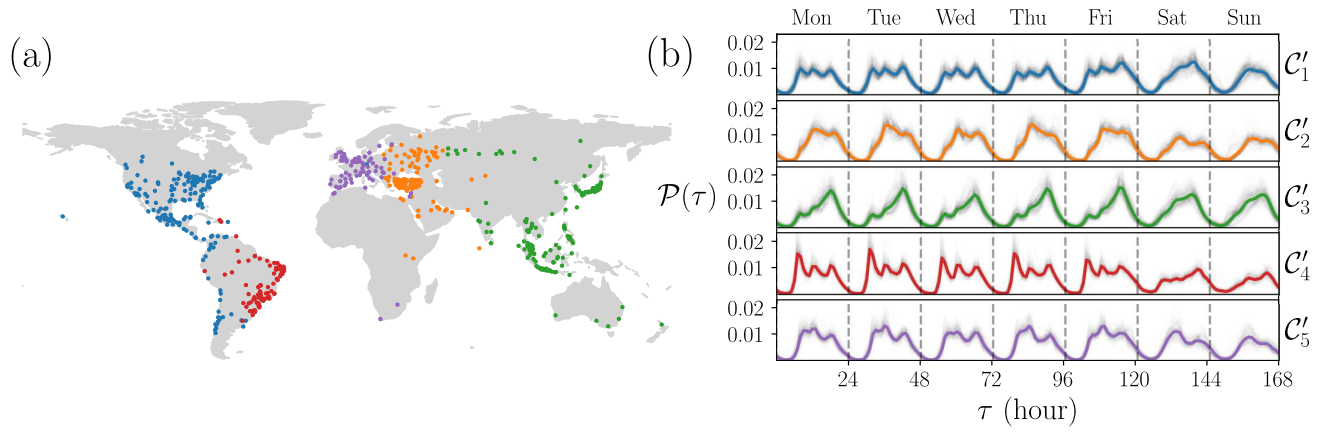


Figure 7. Pattern identification using agglomerative hierarchical clustering. (a) Geographical representation of 5 clusters detected. (b) Activity patterns in each group. All figures were created using python 3.8 and the matplotlib (3.5.0) package (<https://matplotlib.org>). The map in panel (a) was created using the geopandas (0.12.1) package (<https://geopandas.org>).

Once we defined the communities of the network, we can compare the fraction of intra-community and inter-community links. Defining L_s as the number of links between nodes in community \mathcal{C}_s , and L_{st} as the number of links between a node in \mathcal{C}_s and a node in \mathcal{C}_t , we calculate the fraction of inter-community links as $L_{st}/(\mathcal{N}_s\mathcal{N}_t)$ and intra-community links as $2L_s/(\mathcal{N}_s(\mathcal{N}_s-1))$. The values obtained allow us to compare the number of links with the total number of possible links. The values for the fraction of intra-community links are 0.79, 0.68, 0.51, 0.76 and 0.75 for $\mathcal{C}_1, \dots, \mathcal{C}_5$, respectively. Regarding the fraction of inter-community links, the values are below 0.1 except between communities \mathcal{C}_1 and \mathcal{C}_4 (North America and South America) with 0.32 and, with 0.26, between \mathcal{C}_1 and \mathcal{C}_5 (North America and Europe); there are a fraction 0.15 of inter-community nodes between \mathcal{C}_2 (Middle East) and \mathcal{C}_5 (Europe), and 0.12 between \mathcal{C}_5 and \mathcal{C}_4 (South America). The results also show that \mathcal{C}_3 has little similarity with the other communities. Europe is a community with many elements in common with America and the Near East. East Asia, on the other hand, has few elements in common with the rest of the world in terms of temporal patterns of human behavior. These features are observed in the map in Fig. 6(c) evidencing cultural and historical features of each region.

Finally, it is worth mentioning that, unlike other cluster identification methods, e.g., agglomerative clustering (discussed in the next section), information on similarity between specific regions within the same communities is preserved in the individual links. In Fig. 6(c), it is clear the high density of links between North America and United Kingdom, as well as Brazil and Portugal, regions with cultural and linguistic relationships. The results also show that not all cities belong to the same community as would be expected based on their geographic region. Specifically, there are 8 cities in Chile, 3 in Mexico and 1 in Uruguay that are more similar to European cities than to American ones.

Identification of patterns using machine learning

Machine learning can be used as an alternative approach, with many algorithms involved, to classify objects or patterns in a very efficient way^{47,56}. In particular, we used the unsupervised hierarchical agglomerative clustering to classify our temporal patterns of activity in cities. When we apply this algorithm to our data set, we obtained five clusters, as shown in Fig. 7. This number of clusters or communities is obtained by maximizing the modularity. The clusters of cities detected are presented in Fig. 7(a). For comparison, these clusters are depicted using the same colors as those used in Fig. 6(c). In this classification of the dataset of check-ins, each cluster obtained by this procedure is denoted as \mathcal{C}'_s and contains \mathcal{N}'_s elements (with $s = 1, 2, \dots, 5$). We have: $\mathcal{N}'_1 = 178$, $\mathcal{N}'_2 = 128$, $\mathcal{N}'_3 = 140$, $\mathcal{N}'_4 = 90$, and $\mathcal{N}'_5 = 87$. A comparison of Fig. 7(a) and our findings in Fig. 6(c) shows that the differences between \mathcal{N}_s and \mathcal{N}'_s are mainly due to cities from South America and the Caribbean that were in \mathcal{C}_1 (blue) are now in \mathcal{C}'_4 (red), and between Russian and Indian cities that were in \mathcal{C}_2 (orange) now belong to \mathcal{C}'_3 (green). In addition, Fig. 7(b) shows the probabilities $\mathcal{P}_i(\tau)$ grouped according to this classification. Again, in each panel, corresponding \mathcal{C}'_s , the \mathcal{N}'_s curves of the cities are shown in thin gray, while the average behavior for each time τ is shown with a colored thick line. The resemblance to the behaviors shown in Fig. 7(b) is remarkable showing that the emergent patterns in the dataset can be detected by different algorithms.

Discussion

In this work, we use Foursquare check-ins as a proxy of human activity in cities. The data set explored provide vast information about people's interests, site characteristics, and behavioral patterns in cities, among many others. The information analyzed contains 90,048,627 check-ins made by 2,733,324 users from April 2012 to January 2014 with active check-ins obtained from registers on Twitter by searching a hashtag generated automatically for users that linked their Foursquare activity with that social network. Information from 632 cities from 84 countries, with more than 10,000 POIs, was used. We explore the spatial properties of POIs and check-ins and the temporal features of the check-ins which, as self-reported spatio-temporal interactions between people and places, provide valuable information about activities carried out in cities. In particular, we analyze statistically the check-ins per hour on weeks for each city.

From the probabilities describing the temporal activity of each city, we apply a symmetrized Kullback-Leibler distance to compare these probabilities across all 632 cities. From this information, we define similarity networks in terms of a threshold value H to decide if two cities have a similar activity or not. We explore the size of the largest connecting component as a function of H ; in particular, we found that around $H = 0.02$ a critical percolation threshold exists, whereas for $H = 0.0723$ the largest connected component includes all the nodes of the network. Our findings reveal collective emergent behaviors that go beyond the spatial and mobility aspects that define metropolitan areas, megacities, or functional urban areas, and allows for the tracking of higher-order structures, as was proven in some cities that have great similarity, despite the fact that their geographical separation prevents them from being the same.

We apply Louvain's algorithm for community detection to the similarity network generated with $H = 0.0723$; the results define 5 groups of cities with similar activity of check-ins. By locating all the cities in a map, we notice a remarkable pattern: The five communities of cities belong to five different regions that correspond to different continents. In addition, we use a Machine Learning algorithm to classify the activity patterns obtained. Although this method is completely different from the Network Science approach, we nevertheless obtained basically the same classification. Specifically, the Machine Learning algorithm that we used was the Unsupervised Agglomerating Clustering^{47,56}. Both approaches, although very different, lead to the same classification of five different communities worldwide. Even more surprising, these five communities clearly correspond to five different regions on a planetary scale: 1) North America, (2) South America, (3) West Europe, (4) East Europe and Middle East, and (5) East Asia.

In summary, using a vast data set from location-based social networks, we analyze 632 cities of 84 countries around the world to obtain temporal patterns of human activity that identify points of interest within the cities. Using network science and machine learning algorithms we unravel communities with different patterns of human behaviour. This suggest that human activity patterns can be universal with some geographical, historical and cultural variations on a planetary scale.

Methods

Dataset description

Check-ins information was collected by Yang, et al.^{29,30,35,36} and it is publicly available⁴⁸. The datasets are divided into two sets. The first one is a list of check-ins obtained through an automated search on Twitter with the help of its API streaming service³⁶. Foursquare allows linking users' accounts with other social media such as Twitter or Facebook, to share the check-ins on these platforms too. If this is the case, when one user registers their presence in a place, automatically, a tweet or a post is generated with the information of the check-in and some elements like hashtags and the URL of the venue's page at Foursquare. Although the users that link their accounts in this way are only a subset of all the Foursquare users, this dataset contains information on about 2,733,324 users made in almost 22 months (from April 4, 2012, to January 29, 2014). With the information of tweets, a check-in dataset D_{45} was made with 90,048,627 rows, each one corresponding to a check-in, i.e. the interaction between a user, with an anonymized ID, and a POI, where the ID is an alphanumeric identifier of the site in the Foursquare platform. Each record includes the Coordinated Universal Time (UTC) when the check-in occurred and the fourth column is the correction of the UTC corresponding to the Time Zone where the check-in was made. The user ID data has 2,733,324 different values, which corresponds to the activity of the same number of users. The POI ID column has 11,180,160 different values, which is equivalent to the number of POIs in the dataset.

From the information in the tweets, it is possible to obtain the POI profile from Foursquare's site and with it the information contained in the second dataset, D_{POI} . Each POI ID is the same alphanumeric code that appears in D_{45} ; this column contains 11,180,160 different values. In addition, each place is described by its geographical coordinates: latitude, and longitude, described by floating numbers that obey the World Geodetic System 1984 standard (WGS84) with 6 decimal places, which is equivalent to a precision of less than one meter. Each POI is described by a category name; the dataset contains 519 different categories of which "Home (private)" is the most common with 1,310,012 sites, followed by "Residential Building (Apartment

Country		POIs		Check-ins		Users
Code	Name	Number	%	Number	%	Number
US	United States	1990327	17.80	12778097	14.19	426341
ID	Indonesia	1198611	10.72	7765315	8.62	361193
BR	Brazil	1159258	10.37	9991354	11.10	261079
TR	Turkey	1098373	9.82	17500113	19.43	592630
RU	Russia	546532	4.89	4291601	4.77	122268
JP	Japan	519409	4.65	4784080	5.31	81293
MY	Malaysia	493453	4.41	4926145	5.47	127390
MX	Mexico	408434	3.65	3981409	4.42	147563
TH	Thailand	353444	3.16	2633608	2.92	82765
PH	Philippines	219097	1.96	1998063	2.22	60197
ES	Spain	212161	1.90	1083153	1.20	67638
GB	United Kingdom	210777	1.89	1271622	1.41	77949
IT	Italy	197007	1.76	867931	0.96	52394
CL	Chile	195226	1.75	2209981	2.45	53714
DE	Germany	142347	1.27	623759	0.69	45574

Table 1. Foursquare data set by country. The first 15 countries sorted by the number of points of interest (POI) are shown, as well as the number of check-ins, users, and the percentage of the total dataset that represents.

/ Condo)” with 354,858; the third most popular is “Office” with 317,149; the fourth place is occupied by “Building” with 255,121 sites; the following are “Café”, “Restaurant”, “Bar” and “Hotel” with 188436, 153027, 145878 and 138476 sites, respectively. This information also includes the country code of the POI according to the two-letter ISO 3166-1 standard; containing 253 different codes. Then, the dataset includes check-in on every country in the World. From the 253 country codes, 84 countries with 5000 POIs or more represent 98.92% of the data. Using the information in the country code, we group all the POIs by their code, obtaining 253 datasets, $D_{POI}(\text{code})$, each containing the POIs of a single country. In Table 1, 15 countries with most of the POIs are listed; 80% of the venues belong to these countries. From this, we can highlight the presence of countries with remarkable diversity in terms of culture and geography.

With the information of each set $D_{POI}(\text{code})$, D_{AS} can be filtered, grouping the check-ins by country code. In this manner, it is possible to know the number of check-ins per country and the number of users who had activity in each country, as shown in the Table 1. In addition to the number of POIs and check-ins, this table shows the percentage that this number represents of the total. The same is not done in the case of users since many users have activity in more than one country. Although the order in the ranking varies, the same countries that concentrate the majority of the POIs add up to the largest number of check-ins. Regarding check-ins, the records in the 85 countries that contain 25,000 check-ins or more, represent 99.54% of the data.

Grouping POIs by urban area

Our topic of interest is the behavior of people in cities, so classifying POIs and check-ins by country is not enough. The definition of what a city is and what its borders are is a complex topic and has been dealt with by different authors^{3,57,58}. In this work, we opt for the definition of *Functional Urban Area* used by the European Commission, which integrates factors such as infrastructure, population, and economy, and with which the Joint Research Centre generated the Global Human Settlement – Urban Centre Database (GHS), a dataset with the borders of 13,135 urban areas worldwide. This information is contained in a shapefile publicly available⁵⁹ that includes the name of the city, its population, coordinates, area, the country, and region in which it is located, if it extends beyond the borders of a single region within the same country (New York, whose functional urban area is divided into counties belonging to the states of New York and New Jersey, in the United States) or even in more than one country (for example, Detroit, in the United States, whose functional urban area extends to Ontario, Canada, including the city of Windsor); among much more information. We use this dataset to group POIs by functional urban areas using Geopandas, a Python package for data analysis with geographic information⁶⁰. Of all the urban areas contained in the GHS, 6,463 cities have, at least, one Foursquare POI. The POIs that are located within these cities represent 74 percent of the total; 82% of the total check-ins were carried out in them. We focused on the 632 urban areas that have more than 10,000 check-ins, which represent 63% of the total POIs (7,026,688), and 76% of the total check-ins (68,356,896). That is, more than three-quarters of the total check-ins in the database were made in urban areas with more than 10,000 check-ins. The 31 cities with more records are shown in Table 2. Again, we find great diversity in cultural, social, and geographic terms, giving

City	Country	POIs	Check-ins	POIs / km ²	Check-ins PC
Istanbul	TR	334517	7343552	249.640	0.520404
Jakarta	ID	398154	2908026	79.488	0.080083
Kuala Lumpur	MY	200199	2558716	150.752	0.403605
Tokyo	JP	191162	2405876	35.946	0.072842
Mexico City	MX	137655	1804660	65.116	0.092265
Bangkok	TH	169220	1741638	65.896	0.118231
Moscow	RU	160868	1643199	85.477	0.116726
São Paulo	BR	137494	1478616	68.576	0.077356
Izmir	TR	74237	1443711	210.303	0.516692
Quezon City [Manila]	PH	123941	1343955	61.055	0.061959
New York	US	137841	1311179	25.602	0.082202
Santiago	CL	89115	1276748	123.771	0.201507
Ankara	TR	59610	1021287	158.537	0.340152
Bandung	ID	119357	933686	117.709	0.114121
Singapore	SG	72981	827715	83.027	0.119596
Surabaya	ID	110852	756628	63.308	0.090586
Los Angeles	US	91011	698605	16.157	0.048916
Osaka [Kyoto]	JP	66574	667631	21.081	0.042544
Yogyakarta	ID	83635	609749	53.785	0.119592
Rio de Janeiro	BR	55765	570441	40.794	0.058220
Belém	BR	39125	490162	143.842	0.234762
Chicago	US	55319	485198	14.444	0.071565
Saint Petersburg	RU	56800	482715	107.780	0.112237
Kuwait City	KW	43547	473904	91.485	0.149590
London	GB	48778	430524	26.168	0.044801
Lima	PE	34989	404408	39.942	0.043646
Denpasar	ID	54399	393148	130.453	0.209318
Bursa	TR	25214	392454	120.067	0.233577
Manaus	BR	34633	390084	132.693	0.193399
Medan	ID	46528	387255	62.961	0.097886
Seoul	KR	79306	382646	32.383	0.017714

Table 2. Foursquare data by city. The 31 cities with the highest number of check-ins are shown. This selection contains information on a wide variety of countries with different geographic, cultural, linguistic, economic, and religious characteristics.

the Foursquare dataset great relevance for the study of urban dynamics. Along with the number of check-ins, the number of POIs per square kilometer and the number of check-ins per city inhabitant were calculated to give us an idea of the urban environments reflected by the Foursquare activity.

References

1. Batty, M. *The new science of cities* (MIT press, 2013).
2. Barthelemy, M. *The structure and dynamics of cities* (Cambridge University Press, 2016).
3. Bettencourt, L. M. *Introduction to urban science: evidence and theory of cities as complex systems* (MIT Press, 2021).
4. Shi, W., Goodchild, M., Batty, M., Kwan, M. & Zhang, A. *Urban Informatics*. The Urban Book Series (Springer Nature Singapore, 2021).
5. Brockmann, D., Hufnagel, L. & Geisel, T. The scaling laws of human travel. *Nature* **439**, 462, DOI: [10.1038/nature04292](https://doi.org/10.1038/nature04292) (2006).
6. Sobolevsky, S. *et al.* Cities through the prism of people's spending behavior. *PLoS One* **11**, e0146291, DOI: [10.1371/journal.pone.0146291](https://doi.org/10.1371/journal.pone.0146291) (2016).
7. Jiang, S., Ferreira, J. & González, M. C. Clustering daily patterns of human activities in the city. *Data Min. Knowl. Discov.* **25**, 478–510, DOI: [10.1023/a:1014247822322](https://doi.org/10.1023/a:1014247822322) (2012).

8. Sim, A., Yaliraki, S. N., Barahona, M. & Stumpf, M. P. Great cities look small. *J. R. Soc. Interface* **12**, 20150315, DOI: [10.1098/rsif.2015.0315](https://doi.org/10.1098/rsif.2015.0315) (2015).
9. Lenormand, M., Bassolas, A. & Ramasco, J. J. Systematic comparison of trip distribution laws and models. *J. Transp. Geogr.* **51**, 158–169, DOI: [10.1016/j.jtrangeo.2015.12.008](https://doi.org/10.1016/j.jtrangeo.2015.12.008) (2016).
10. Sun, L., Axhausen, K. W., Lee, D.-H. & Cebrian, M. Efficient detection of contagious outbreaks in massive metropolitan encounter networks. *Sci. Rep.* **4**, 1–6, DOI: [10.1038/srep05099](https://doi.org/10.1038/srep05099) (2014).
11. Riascos, A. P. & Mateos, J. L. Networks and long-range mobility in cities: A study of more than one billion taxi trips in New York City. *Sci. Rep.* **10**, 4022, DOI: [10.1038/s41598-020-60875-w](https://doi.org/10.1038/s41598-020-60875-w) (2020).
12. Melikov, P. *et al.* Characterizing Urban Mobility Patterns: A Case Study of Mexico City. In *Urban Informatics*, 153–170 (Springer, 2021).
13. McKenzie, G. & Romm, D. Measuring urban regional similarity through mobility signatures. *Comput. Environ. Urban Syst.* **89**, 101684, DOI: [10.1016/j.compenvurbsys.2021.101684](https://doi.org/10.1016/j.compenvurbsys.2021.101684) (2021).
14. Blondel, V. D., Decuyper, A. & Krings, G. A survey of results on mobile phone datasets analysis. *EPJ Data Sci.* **4**, 10, DOI: [10.1140/epjds/s13688-015-0046-0](https://doi.org/10.1140/epjds/s13688-015-0046-0) (2015).
15. González, M. C., Hidalgo, C. A. & Barabási, A.-L. Understanding individual human mobility patterns. *Nature* **453**, 779–782, DOI: [10.1038/nature06958](https://doi.org/10.1038/nature06958) (2008).
16. Song, C., Koren, T., Wang, P. & Barabási, A.-L. Modelling the scaling properties of human mobility. *Nat. Phys.* **6**, 818–823, DOI: [10.1038/nphys1760](https://doi.org/10.1038/nphys1760) (2010).
17. Louail, T. *et al.* From mobile phone data to the spatial structure of cities. *Sci. Rep.* **4**, 5276, DOI: [10.1038/srep05276](https://doi.org/10.1038/srep05276) (2014).
18. Louail, T. *et al.* Uncovering the spatial structure of mobility networks. *Nat. Commun.* **6**, 6007, DOI: [10.1038/ncomms7007](https://doi.org/10.1038/ncomms7007) (2015).
19. Çolak, S., Lima, A. & González, M. C. Understanding congested travel in urban areas. *Nat. Commun.* **7**, 10793, DOI: [10.1038/ncomms10793](https://doi.org/10.1038/ncomms10793) (2016).
20. Alessandretti, L., Sapiezynski, P., Sekara, V., Lehmann, S. & Baronchelli, A. Evidence for a conserved quantity in human mobility. *Nat. Hum. Behav.* **2**, 485–491, DOI: [10.1038/s41562-018-0364-x](https://doi.org/10.1038/s41562-018-0364-x) (2018).
21. Song, C., Qu, Z., Blumm, N. & Barabási, A.-L. Limits of predictability in human mobility. *Science* **327**, 1018–1021, DOI: [10.1126/science.117717](https://doi.org/10.1126/science.117717) (2010).
22. Zhao, K., Musolesi, M., Hui, P., Rao, W. & Tarkoma, S. Explaining the power-law distribution of human mobility through transportation modality decomposition. *Sci. Rep.* **5**, 9136, DOI: [10.1038/srep09136](https://doi.org/10.1038/srep09136) (2015).
23. Pappalardo, L. & Simini, F. Data-driven generation of spatio-temporal routines in human mobility. *Data Min. Knowl. Discov.* **32**, 787–829, DOI: [10.1007/s10618-017-0548-4](https://doi.org/10.1007/s10618-017-0548-4) (2018).
24. Alessandretti, L., Aslak, U. & Lehmann, S. The scales of human mobility. *Nature* **587**, 402–407, DOI: [10.1038/s41586-020-2909-1](https://doi.org/10.1038/s41586-020-2909-1) (2020).
25. Bhattacharya, K. & Kaski, K. Social physics: uncovering human behaviour from communication. *Adv. Physics: X* **4**, 1527723, DOI: [10.1080/23746149.2018.1527723](https://doi.org/10.1080/23746149.2018.1527723) (2019).
26. Bao, J., Zheng, Y., Wilkie, D. & Mokbel, M. Recommendations in location-based social networks: a survey. *GeoInformatica* **19**, 525–565, DOI: [10.1007/s10707-014-0220-8](https://doi.org/10.1007/s10707-014-0220-8) (2015).
27. Chen, Z. *et al.* Contrasting social and non-social sources of predictability in human mobility. *Nat. Commun.* **13**, 1–9, DOI: [10.1038/s41467-022-29592-y](https://doi.org/10.1038/s41467-022-29592-y) (2022).
28. Lenormand, M., Gonçalves, B., Tugores, A. & Ramasco, J. J. Human diffusion and city influence. *J. The Royal Soc. Interface* **12**, 20150473, DOI: [10.1098/rsif.2015.0473](https://doi.org/10.1098/rsif.2015.0473) (2015).
29. Yang, D., Fankhauser, B., Rosso, P. & Cudre-Mauroux, P. Location prediction over sparse user mobility traces using rnns: Flashback in hidden states! In *Proceedings of the Twenty-Ninth International Joint Conference on Artificial Intelligence*, 2184–2190 (2020).
30. Yang, D., Qu, B., Yang, J. & Cudre-Mauroux, P. Revisiting user mobility and social relationships in LBSN: A hypergraph embedding approach. In *The world wide web conference*, 2147–2157 (2019).

31. Riascos, A. P. & Mateos, J. L. Emergence of encounter networks due to human mobility. *PLoS One* **12**, e0184532, DOI: [10.1371/journal.pone.0184532](https://doi.org/10.1371/journal.pone.0184532) (2017).
32. Foursquare City Guide. <https://foursquare.com/city-guide>.
33. Noulas, A., Scellato, S., Lambiotte, R., Pontil, M. & Mascolo, C. A tale of many cities: universal patterns in human urban mobility. *PLoS One* **7**, e37027, DOI: [10.1371/journal.pone.0037027](https://doi.org/10.1371/journal.pone.0037027) (2012).
34. Yang, D., Zhang, D., Zheng, V. W. & Yu, Z. Modeling user activity preference by leveraging user spatial temporal characteristics in lbsns. *IEEE Trans. Syst. Man Cybern.: Syst.* **45**, 129–142, DOI: [10.1109/TSMC.2014.2327053](https://doi.org/10.1109/TSMC.2014.2327053) (2015).
35. Yang, D., Qu, B., Yang, J. & Cudré-Mauroux, P. Lbsn2vec++: Heterogeneous hypergraph embedding for location-based social networks. *IEEE Trans. Knowl. Data Eng.* DOI: [10.1109/TKDE.2020.2997869](https://doi.org/10.1109/TKDE.2020.2997869) (2020).
36. Yang, D., Qu, B. & Cudre-Mauroux, P. Location-centric social media analytics: Challenges and opportunities for smart cities. *IEEE Intell. Syst.* **36**, 3–10, DOI: [10.1109/MIS.2020.3009438](https://doi.org/10.1109/MIS.2020.3009438) (2020).
37. Gallotti, R., Bertagnolli, G. & De Domenico, M. Unraveling the hidden organisation of urban systems and their mobility flows. *EPJ Data Sci.* **10**, 3, DOI: [10.1140/epjds/s13688-020-00258-3](https://doi.org/10.1140/epjds/s13688-020-00258-3) (2021).
38. Noulas, A., Shaw, B., Lambiotte, R. & Mascolo, C. Topological properties and temporal dynamics of place networks in urban environments. In *Proceedings of the 24th International Conference on World Wide Web*, 431–441 (2015).
39. Noulas, A., Scellato, S., Mascolo, C. & Pontil, M. An empirical study of geographic user activity patterns in foursquare. In *Proceedings of the International AAAI Conference on Web and Social Media*, vol. 5-1, 570–573 (2011).
40. Cornacchia, G. & Pappalardo, L. Sts-epr: Modelling individual mobility considering the spatial, temporal, and social dimensions together. *Procedia Comput. Sci.* **184**, 258–265, DOI: <https://doi.org/10.1016/j.procs.2021.03.035> (2021). The 12th International Conference on Ambient Systems, Networks and Technologies (ANT) / The 4th International Conference on Emerging Data and Industry 4.0 (EDI40) / Affiliated Workshops.
41. Barabási, A.-L. The origin of bursts and heavy tails in human dynamics. *Nature* **435**, 207–211, DOI: [10.1038/nature03459](https://doi.org/10.1038/nature03459) (2005).
42. Saramäki, J. & Moro, E. From seconds to months: an overview of multi-scale dynamics of mobile telephone calls. *Eur. Phys. J. B* **88**, 1–10, DOI: [10.1140/epjb/e2015-60106-6](https://doi.org/10.1140/epjb/e2015-60106-6) (2015).
43. Prieto Curiel, R., Patino, J. E., Duque, J. C. & O’Clery, N. The heartbeat of the city. *PLoS One* **16**, e0246714, DOI: [10.1371/journal.pone.0246714](https://doi.org/10.1371/journal.pone.0246714) (2021).
44. Sparks, K., Thakur, G., Pasarkar, A. & Urban, M. A global analysis of cities’ geosocial temporal signatures for points of interest hours of operation. *Int. J. Geogr. Inf. Sci.* **34**, 759–776, DOI: [10.1080/13658816.2019.1615069](https://doi.org/10.1080/13658816.2019.1615069) (2020).
45. Barabási, A. & Pósfai, M. *Network Science* (Cambridge University Press, 2016).
46. Cover, T. & Thomas, J. *Elements of Information Theory*. A Wiley-Interscience publication (Wiley, 2006).
47. Hastie, T., Tibshirani, R. & Friedman, J. *The Elements of Statistical Learning: Data Mining, Inference, and Prediction*. Springer Series in Statistics (Springer New York, 2017).
48. Dingqi YANG’s Homepage. <https://sites.google.com/site/yangdingqi/home/foursquare-dataset>.
49. Ruiz-Gayosso, J. A. & Riascos, A. P. Human mobility in the airport transportation network of the United States. *Int. J. Mod. Phys. C* 2350072, DOI: [10.1142/S0129183123500729](https://doi.org/10.1142/S0129183123500729) (2023).
50. Kullback, S. & Leibler, R. A. On Information and Sufficiency. *The Annals Math. Stat.* **22**, 79 – 86, DOI: [10.1214/aoms/1177729694](https://doi.org/10.1214/aoms/1177729694) (1951).
51. Newman, M. E. J. & Girvan, M. Finding and evaluating community structure in networks. *Phys. Rev. E* **69**, 026113, DOI: [10.1103/PhysRevE.69.026113](https://doi.org/10.1103/PhysRevE.69.026113) (2004).
52. Newman, M. E. J. Modularity and community structure in networks. *Proc. Natl. Acad. Sci. U.S.A.* **103**, 8577–8582, DOI: [10.1073/pnas.0601602103](https://doi.org/10.1073/pnas.0601602103) (2006).
53. Fortunato, S. Community detection in graphs. *Phys. Rep.* **486**, 75–174, DOI: [10.1016/j.physrep.2009.11.002](https://doi.org/10.1016/j.physrep.2009.11.002) (2010).
54. Blondel, V. D., Guillaume, J.-L., Lambiotte, R. & Lefebvre, E. Fast unfolding of communities in large networks. *J. Stat. Mech: Theory Exp.* **2008**, P10008, DOI: [10.1088/1742-5468/2008/10/p10008](https://doi.org/10.1088/1742-5468/2008/10/p10008) (2008).
55. NetworX - Network Analysis in Python. <https://networkx.org/>.
56. Müller, A. & Guido, S. *Introduction to Machine Learning with Python: A Guide for Data Scientists* (O’Reilly Media, 2016).

57. Rozenfeld, H. D. *et al.* Laws of population growth. *Proc. Natl. Acad. Sci.* **105**, 18702–18707, DOI: [10.1073/pnas.0807435105](https://doi.org/10.1073/pnas.0807435105) (2008).
58. Ortman, S. G., Lobo, J. & Smith, M. E. Cities: Complexity, theory and history. *PLoS One* **15**, e0243621, DOI: [10.1371/journal.pone.0243621](https://doi.org/10.1371/journal.pone.0243621) (2020).
59. Florczyk, A. J. *et al.* GHS Urban Centre Database 2015, multitemporal and multidimensional attributes, r2019a. *Eur. Comm. Jt. Res. Centre (JRC)[Dataset]*. Available online <https://data.jrc.ec.europa.eu/dataset/53473144-b88c-44bc-b4a3-4583ed1f547e> (accessed on May 2022) (2019).
60. Jordahl, K. *et al.* geopandas/geopandas: v0.8.1, DOI: [10.5281/zenodo.3946761](https://doi.org/10.5281/zenodo.3946761) (2020).

Acknowledgements

F.B. acknowledges support from CONACYT México. This work was supported by PAPIIT-UNAM grant No. IN116220.

Author contributions statement

F.B., A.P.R. and J.L.M. designed the research, performed the research, and wrote the manuscript.